Hindawi
International Journal of Antennas and Propagation
Volume 2023, Article ID 8865793, 13 pages
https://doi.org/10.1155/2023/8865793

Research Article

Investigation of Planar Isolators for Mutual Coupling Reduction in Two-Dimensional Microstrip Antenna Arrays

Ruowei Yin and Zhipeng Wu

Department of Electrical and Electronic Engineering, University of Manchester, M13 9PL, Manchester, UK

Correspondence should be addressed to Zhipeng Wu; zhipeng.wu@manchester.ac.uk

Received 20 March 2023; Revised 4 July 2023; Accepted 8 July 2023; Published 25 July 2023

Academic Editor: Trushit Upadhyaya

The design of isolators to reduce mutual coupling in large two-dimensional antenna arrays is complex and requires significant computational effort. This work attempts to alleviate this problem by applying different types of planar isolators in different orientations and experimenting first with two-element microstrip antenna arrays. A U-shaped planar transmission line isolator, a U-shaped planar transmission line-based destructive ground structure, and a planar neutralization line structure are designed to reduce E-plane or H-plane coupling in two-element microstrip antenna arrays. A mutual coupling reduction of approximately 6 dB is achieved. Four combinations of these planar isolators are compared and analyzed in a four-element microstrip antenna array. An optimal combination is then obtained by using two reversely placed U-shaped line isolators, which reduce the mutual coupling by more than 6.1 dB. The study is also extended to a 5×5 antenna array. Similar results of mutual coupling reduction are obtained. In addition to simulation, both two-element and 25-element microstrip antennas have been constructed and tested. The agreement of the simulation results with the measured results confirms the effectiveness of the decoupling structures.

1. Introduction

Multiple-input multiple-output (MIMO) technology uses multiple antennas to significantly increase the system's data throughput [1, 2] and transmission rate [3, 4] without additional bandwidth. It has been used in 5G wireless communication systems and future wireless communications. However, the increasing number of antenna elements and limited spacing aggravate the mutual coupling problem. Mutual coupling results in impedance mismatching [5] and radiation pattern distortion, degrading system performance [6, 7]. Therefore, improving the isolation between antennas becomes increasingly important.

Several decoupling techniques have been proposed to achieve low mutual coupling, such as resonant isolators [8–10], neutralization structures [11, 12], electromagnetic bandgap (EBG) [13, 14], and frequency-selective surface (FSS) structures [15–17]. However, the studies of these structures are limited to two-element or one-dimensional (1D) antenna arrays, which reduce the coupling on E-plane or H-plane only.

For two-dimensional (2D) antenna arrays, both H-coupling and E-coupling exist, which increases the isolator design complexity. A double-layer meta-surface superstrate [18] and an array-antenna decoupling surface (ADS) [19] have been proposed to reduce the mutual coupling by placing the structures above the antenna arrays. The superstructure generates reflected waves that can cancel surface wave coupling by varying the pattern of the reflective metal sheets on the superstructure. A cross-shaped metal wall [20] and a metamaterial absorber wall [21] have been investigated to suppress the surface wave coupling. The metamaterial wall absorbs part of the coupled electromagnetic wave energy, thus reducing the coupling between the antennas. However, these isolators [18–21] have a high profile due to the additional height of the superstrates or

walls. In addition, the isolators are designed for specific antenna arrays; the change in the isolator is required to work in antenna arrays of different scales. Transmission-line-based decoupling structures [22, 23] could effectively reduce the mutual coupling by analyzing the impedance performance at port interfaces and choosing all the transmission-line parameters. The isolators [22] designed in a four-element antenna array have been extended to large-scale antenna arrays. However, the parameters of the transmission lines would need to be altered for different scales of antenna arrays. Destructive ground structures (DGSs) have been investigated for the reduction of mutual coupling by changing the current distributions, and an H-shaped DGS has been studied in a four-port microstrip antenna array [24]. In [25], the isolation is enhanced by adjusting the shape of the ground plane under the antenna array, but with a limitation on practical implementation. A decoupling slot-strip array (DSSA) has been shown in [26]. The DSSA consists of a slot array etched on the ground plane and a strip array printed on the patch plane. The DSSA interferes with the current distribution and reduces the mutual coupling to less than −30 dB in a four-element antenna array. However, the same isolator could only provide an isolation lower than −16 dB in a 4×4 antenna array.

The design of isolators in large 2D antenna arrays is complex. In general, the isolators designed in small-scale antenna arrays, such as 2×2 antenna arrays, need to be modified to have similar isolation enhancements in large antenna arrays. This paper hence addresses the problem by adopting a combination of different isolators and orientations. Isolators designed in a two-element antenna array can then be extended to work in a large-scale antenna array and maintain similar level of coupling reduction without changing the size, which simplifies the design complexity. The isolators proposed include a U-shaped planar transmission line isolator, a U-shaped planar transmission line-based DGS, and a planar neutralization line structure. The study of their effectiveness in the reduction of mutual coupling extends from a 2×2 microstrip antenna array to a 5×5 microstrip antenna array. Further details are presented below.

In Section 2, a U-shaped transmission line isolator and a U-shaped transmission line-based DGS are described to reduce E-plane coupling and a neutralization line structure to reduce H-plane coupling in two-element microstrip antenna arrays. In Section 3, a comparison will be made on the combinations of abovementioned three types of isolators on improving isolation in a 2×2 microstrip antenna array. In Section 4, the study will be extended to a 5×5 microstrip antenna array with the optimal combination found in Section 3. Conclusions will be drawn in Section 4.

2. Isolator Design for Two-Element Microstrip Antenna Arrays

2.1. Horizontally Placed Two-Element Array. Patch antennas are widely used in base stations because of their low profile, low cost, and easy-to-manufacture performance. Therefore, the microstrip antenna is chosen as the reference antenna. Figure 1(a) shows two identical microstrip antennas of length (L) 19.22 mm and width (W) 26.30 mm placed horizontally on an FR-4 substrate. The edge-to-edge distance (S) is 21.40 mm ($\lambda/4$). This coupling between two horizontally placed microstrip antennas is noted as H-plane coupling.

To investigate isolators in different orientations later, a noncentrosymmetric U-shaped planar transmission line isolator is then introduced between the antennas, as shown in Figure 1(b). This isolator structure is an extended design inspired by the work of a U-shaped resonant isolator [27]. The isolator consists of four symmetrically placed U-shaped lines. It has an overall width (X) and length (Y) which are chosen to be 13.00 mm and 36.00 mm, respectively. The width of lines (a) and the gap between lines (g) are both 0.3 mm.

The U-shaped line isolator can be considered as a band-stop filter. The operating mechanism of the isolator is that the incident electric field is perpendicular to the gap between the U-shaped lines, acting as a capacitor. Conversely, perpendicular to the surface, the H-field introduces inductance. The lengths and gaps can be varied to change the resonant frequency with the changing inductance and capacitance. The electric field intensity at the end of the U-shaped lines is high. When the lines are placed in reverse, the difference in electric field strength is larger; therefore, the capacitance between two adjacent lines is larger. A smaller total inductance is then required to have the same resonant frequency, which means the arms of the U-shaped lines could be shorter, leading to a smaller total size of the isolator. The U-shaped line isolator could be further modified by removing a part of the ground plane.

A DGS-based U-shaped line isolator is shown in Figure 1(c) where the top layer is shown in red and the ground is grey. A part of the ground plane with length (Xslot) 16 mm and width (Yslot) 48 mm is removed. A U-shaped line isolator with a width ($X1$) of 14.5 mm and a length ($Y1$) of 38 mm is then printed on the area at the back side of the FR-4 substrate. The width of the lines ($a1$) and the gap between lines ($g1$) are both 0.7 mm. The defects in the ground layer increase the length of the coupling current path and suppress unwanted surface waves. They provide band-stop filtering characteristics around 3.58 GHz. The coupling current generated by the strip array can offset the coupling current generated by the excitation current.

Taking the two-element microstrip array without an isolator as a reference, Figure 2 shows the simulated results of $|S_{11}|$ and $|S_{21}|$ parameters between two microstrip antennas with the introduction of the isolators above. The reference antenna has a matching frequency of 3.58 GHz. The $|S_{21}|$ value at 3.58 GHz is −22 dB. With the introduction of the U-shaped line isolator and DGS-based U-shaped line isolator, the simulated $|S_{21}|$ values at 3.58 GHz are reduced to −27 dB and −27.5 dB, respectively. The isolation is improved by 5 dB and 5.5 dB, respectively, in simulation. When the antenna array and isolators are fabricated and tested, the measured results are also shown in Figure 2. For the reference antenna, the measured value of $|S_{11}|$ is −33 dB at 3.58 GHz and the measured value of $|S_{21}|$ is −22 dB at

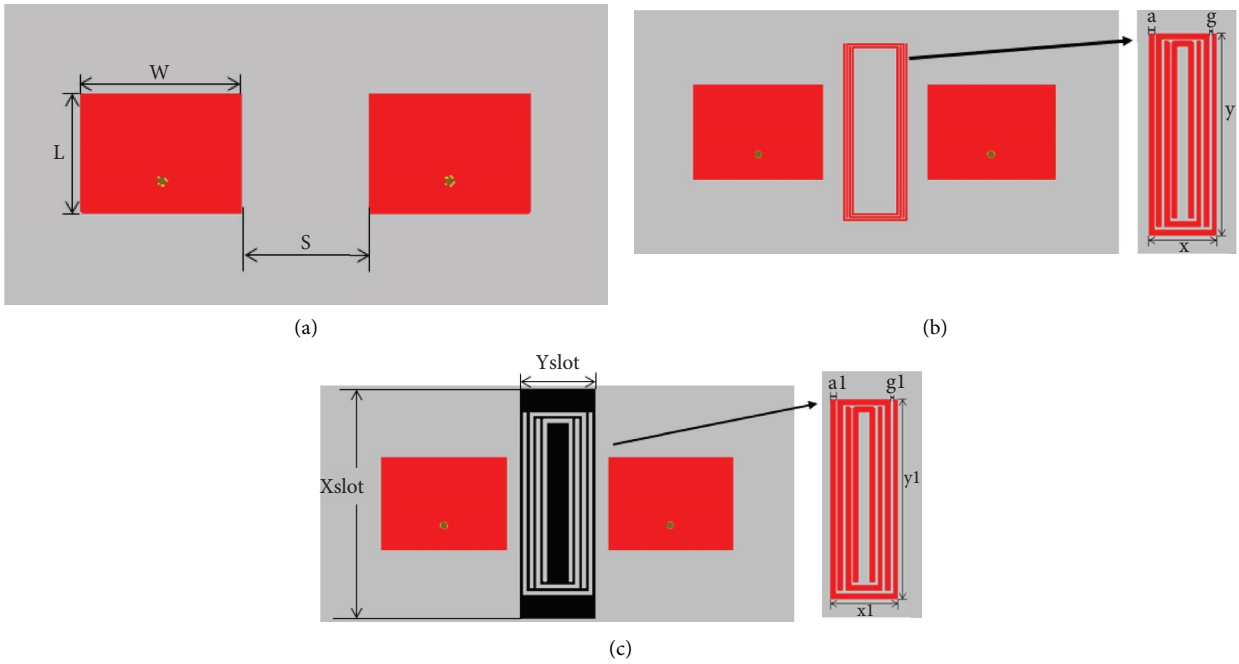

FIGURE 1: The prototype of antenna arrays: (a) horizontally placed antenna array, (b) antenna array with the U-shaped line isolator, and (c) antenna array with the DGS.

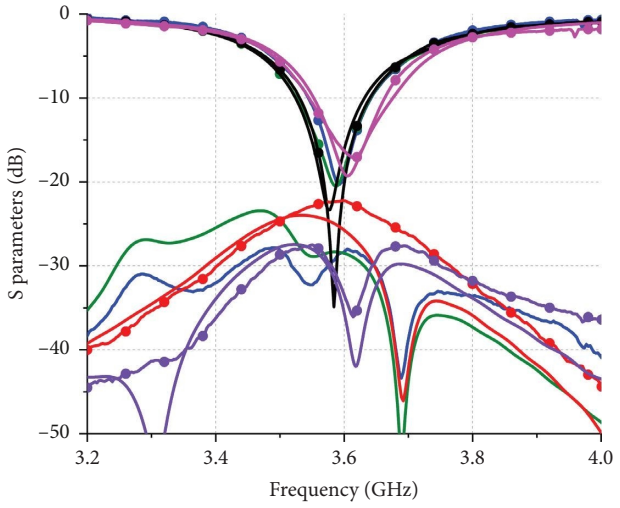

FIGURE 2: Simulated and measured S-parameters for horizontally placed antenna arrays with and without isolators.

3.58 GHz. The measurements also show that the U-shaped line isolator can decrease $|S_{21}|$ to lower than −28.8 dB and DGS-based U-shaped line isolator can decrease to lower than −28.4 dB in the operating region. The isolation is improved by 6.8 dB and 6.4 dB, respectively, consistent with those obtained by simulation.

2.2. Vertically Placed Two-Element Array. When two identical microstrip antennas are placed vertically with $\lambda/4$ edge-to-edge distance in spacing, as shown in Figure 3(a), a simple neutralization line can effectively enhance isolation, as shown in Figure 3(b). The neutralization line has a length of 19 mm and a width of 4.5 mm, and it is inserted in between the microstrip antennas to produce an induced coupling with around 180° phase difference to the direct coupling between them, thereby reducing the overall coupling. Figure 4 shows the simulated and measured $|S_{11}|$ and $|S_{21}|$ results of the antenna array with and without the neutralization line. Both simulation and measurement give similar results, apart from a slight frequency shift. The measured $|S_{11}|$ and $|S_{21}|$ without isolator are −29 dB and −24 dB at the matching frequency of 3.58 GHz. The neutralization line improves the measured $|S_{21}|$ to −29.7 dB or better over the operating bandwidth.

3. Isolator Design for Four-Element Microstrip Antenna Arrays

Extended from the two-element microstrip antenna array arranged in Section 2, a 2×2 microstrip antenna array is formed, as shown in Figure 5(a), with the edge-to-edge spacing of 21.4 mm between adjacent antennas. For easy description, each antenna in the array is numbered from 1 to 4. The simulated current distribution of the antenna arrays is shown in Figure 5(b) when Antenna 1 is excited while the rest of the antennas are terminated by 50 Ω loads. Since the current distributions are similar over the operating frequency band, only the current distributions at the center frequency of 3.58 GHz are shown. When Antenna 1 is excited, considerable currents are induced onto Antennas 2 and 3, and currents induced onto Antennas 4 are generally weak. Hence, the couplings among diagonal elements are not taken into consideration.

With the choices of isolators, four different combinations of isolators, as shown in Figure 6, are considered to

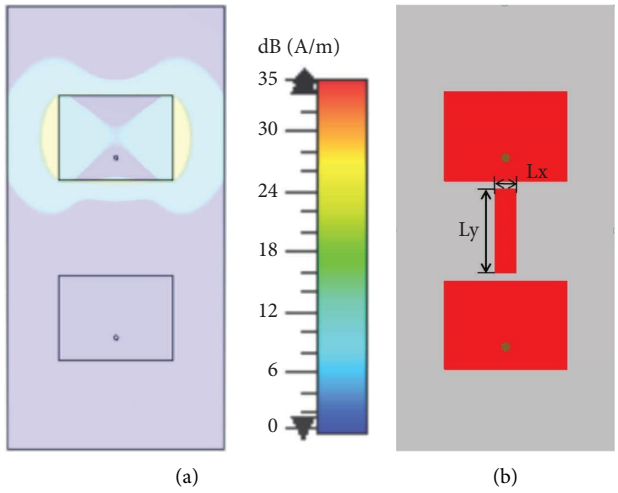

Figure 3: Vertically placed patch antenna array: (a) the surface current distribution of the antenna array and (b) antenna array with a neutralization line.

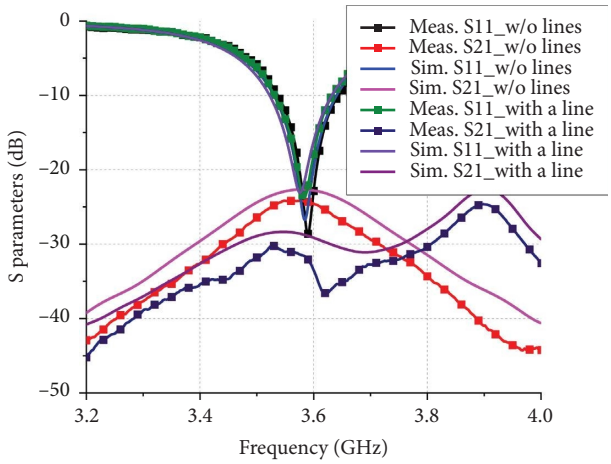

Figure 4: Simulated and measured *S*-parameters for vertically placed antenna array with and without a neutralization line.

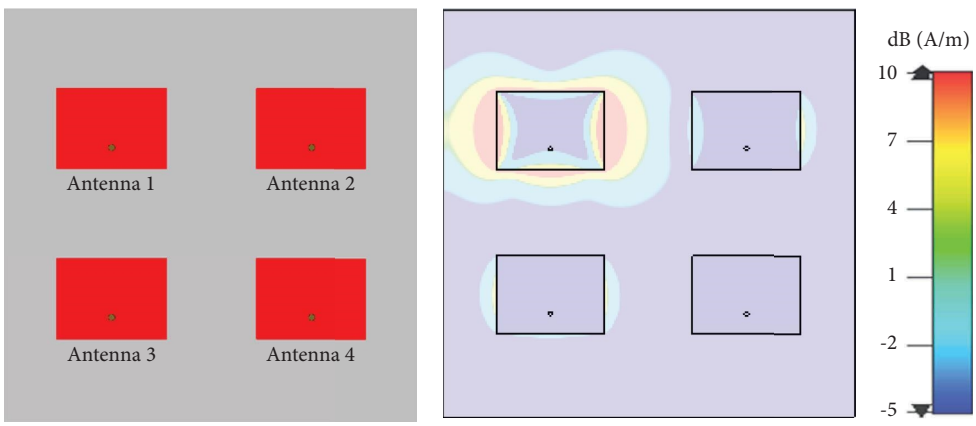

Figure 5: 2 × 2 patch antenna array: (a) structure of the antenna array and (b) the surface current distribution of the antenna array.

show the effect of isolator type and orientation on mutual coupling. These four combinations are listed as follows:

Case 1: two identical U-shaped line isolators and two neutralization lines

Case 2: two reverse-placed U-shaped line isolators and two neutralization lines

Case 3: two reverse-placed U-shaped line-based DGSs and two neutralization lines

Case 4: a line isolator, a U-shaped line-based DGS, and two neutralization lines

With these combinations, the simulated and measured results of S-parameters are shown and compared in Figure 7 together with that without the isolators. Antennas 1 and 4 are chosen as the representative antennas to demonstrate the performance of these four isolator combinations. The responses of S_{21} and S_{34} show the effects of upper and lower isolators, respectively, while S_{31} and S_{24} show the effects of right and left isolators, respectively. The couplings among diagonal elements in the microstrip antenna array are generally weak and hence not taken into consideration. The measured results, also shown in Figure 7, are consistent with the simulated results. It is noted that the reflection coefficients for the arrays are similar, around −20 dB, at the center frequency, and the bandwidths are all around 3%. Their levels of mutual coupling are compared as follows:

The reference antenna array: The maximum H-plane mutual couplings of $|S_{21}|$ and $|S_{34}|$ are −21.6 dB and −23.2 dB, respectively. The maximum E-plane mutual couplings of $|S_{31}|$ and $|S_{24}|$ are −22.9 dB and −23.0 dB, respectively.

Case 1: The maximum H-plane mutual couplings of $|S_{21}|$ and $|S_{34}|$ are −26.9 dB and −27.4 dB, reduced by 5.3 dB and 4.2 dB, respectively. The maximum E-plane mutual couplings of $|S_{31}|$ and $|S_{24}|$ are −28.1 dB and −30.0 dB, reduced by 5.2 dB and 7.0 dB, respectively.

Case 2: The maximum H-plane mutual couplings of $|S_{21}|$ and $|S_{34}|$ are −28.7 dB and −29.3 dB, reduced by 7.1 dB and 6.1 dB, respectively. The maximum E-plane mutual couplings of $|S_{31}|$ and $|S_{24}|$ are −29.0 dB and −29.1 dB, respectively, both reduced by 6.1 dB.

Case 3: The maximum H-plane mutual couplings of $|S_{21}|$ and $|S_{34}|$ are −23.6 dB and −23.9 dB, reduced by 2.0 dB and 0.7 dB, respectively. The maximum E-plane mutual couplings of $|S_{31}|$ and $|S_{24}|$ are −27.8 dB and −29.6 dB, reduced by 4.9 dB and 6.6 dB, respectively.

Case 4: The maximum H-plane mutual couplings of $|S_{21}|$ and $|S_{34}|$ are −26.3 dB and −25.8 dB, reduced by 4.7 dB and 2.6 dB, respectively. The maximum E-plane mutual couplings of $|S_{31}|$ and $|S_{24}|$ are −28.6 dB and −29.2 dB, reduced by 4.9 dB and 5.7 dB, respectively.

The comparison of these four cases shows that the U-shaped line isolator can reduce the coupling by more than 4.2 dB. DGS-based U-shaped line isolator can improve the mutual coupling by over 0.7 dB and the neutralization line by more than 4.9 dB.

The isolator configuration in Case 2 has the best isolation enhancement. In Case 2, the two U-shaped line isolators are placed reversely. Since the U-shaped line isolators are noncentrosymmetric, the reverse placement of the U-shaped line isolators reduces the coupling between the two U-shaped line isolators and hence improved the overall performance.

To further understand the decoupling effect of the isolators, the simulated current distributions of the microstrip antenna arrays with isolators are shown in Figure 8. When antenna 1 is excited, considerable currents are induced onto the upper isolator placed between antennas 1 and 2 and on the left neutralization line between antennas 1 and 3. Due to the distances from other three isolators, the right neutralization line between antennas 2 and 4 has little induced current in all four cases. Individually, for Case 1, the upper line isolator induces a large amount of current to the line isolator between antennas 3 and 4, which degrades the performance of the lower line isolator placed between antennas 1 and 2. For Case 2, only a small amount of current is induced to the lower isolator, thus maintaining the decoupling effect of the lower isolator. For Cases 3 and 4, although the surface current coupled to the bottom isolator is low, the induced current coupled to the upper DGS structure is also very low at 3.5 GHz, which makes the decoupling effect of the upper layer isolator worse and can only reduce less coupling.

The maximum gains of antenna 1 in the four-element microstrip antenna array with and without isolators are given in Figure 9. Both simulation and measurement results show that all four isolator combinations could reduce the gain of the antenna array by up to 0.7 dBi. The measured maximum gain of antenna 1 without isolators is 3.48 dBi at 3.58 GHz. The measured maximum gain at 3.58 GHz of antenna 1 with two U-shaped line isolators (Case 1), that with two reverse-placed U-shaped line isolators (Case 2), that with two DGS-based U-shaped line isolators (Case 3), that with a line isolator, and a DGS-based U-shaped line isolator (Case 4) are 3.23 dBi, 3.05 dBi, 3.42 dBi, and 3.42 dBi, respectively. Four combinations of isolators only reduce the measured gain within 0.43 dBi at 3.58 GHz.

The simulated and measured radiation patterns of the antenna array with and without isolators are shown in Figure 10. The simulated radiation efficiency of Antenna 1 without isolators is 52.6% at 3.58 GHz. The radiation efficiencies of antenna 1 with two U-line isolators (Case 1), antenna 1 with two reversely placed U-line isolators (Case 2), antenna 1 with two DGS-based U-line isolators (Case 3), and antenna 1 with one line isolator and one DGS-based U-line isolator (Case 4) are 46.9%, 48.1%, 53.5%, and 54.2%, respectively. Four combinations of isolators change the efficiency by only 6%. As shown in Figure 10, the back lobe of the antenna array with Case 3 and that with Case 4 is slightly higher due to the variation of ground. Four combinations of isolators have a limited effect on the radiation patterns.

The antenna arrays with and without different types and orientations of isolators are compared in Table 1. Four combinations of isolators have a limited effect on gain and efficiency. Combining a reversely placed U-line isolator and

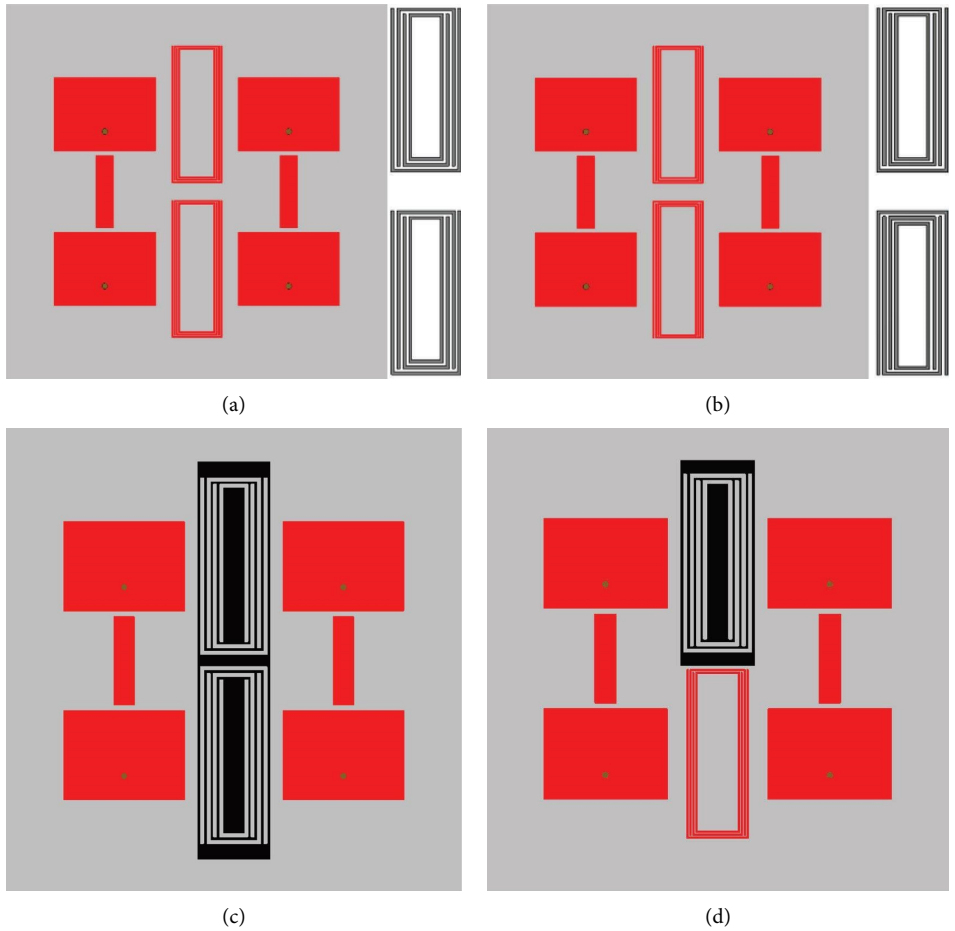

Figure 6: Four-element microstrip antenna arrays: (a) Case 1, (b) Case 2, (c) Case 3, and (d) Case 4.

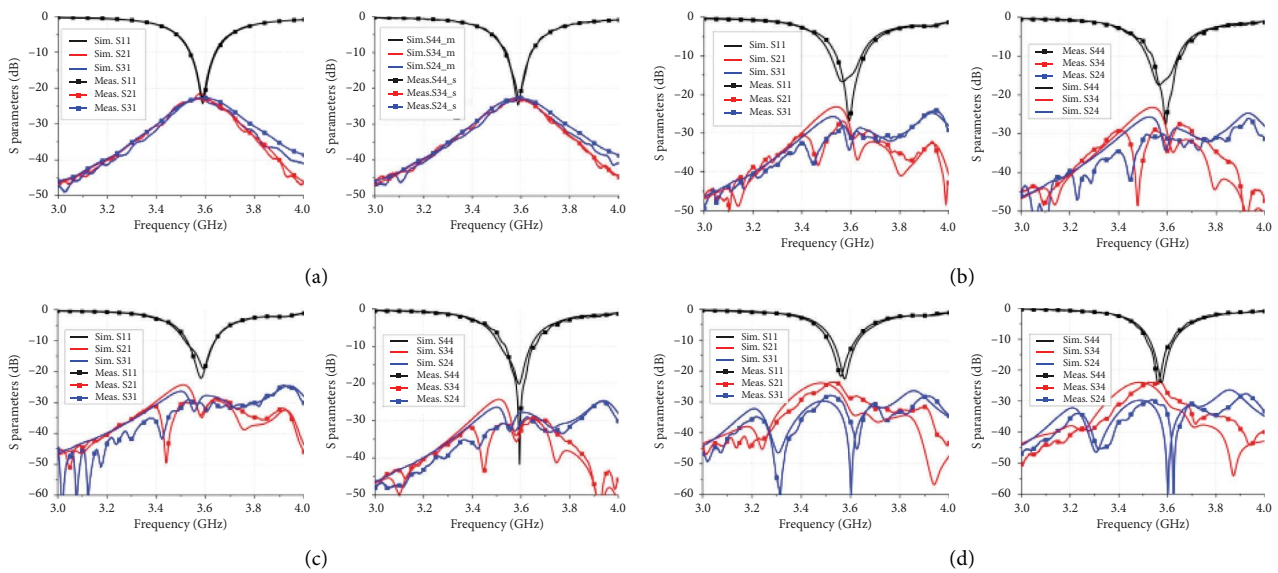

Figure 7: Continued.

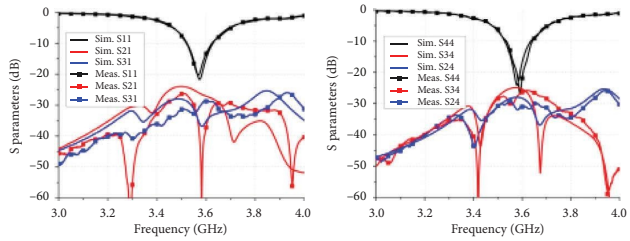

(e)

FIGURE 7: Simulated and measured *S*-parameters of the microstrip antenna arrays: (a) reference antenna array, (b) array with Case 1, (c) array with Case 2, (d) array with Case 3, and (e) array with Case 4.

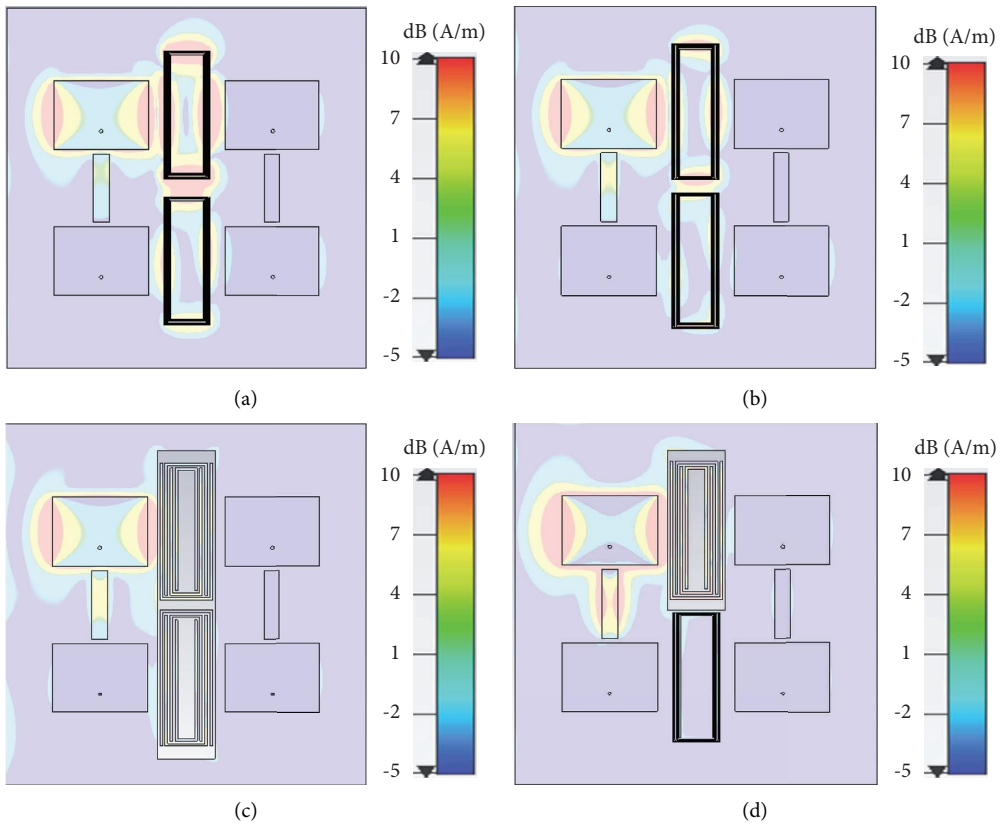

FIGURE 8: Surface currents on the microstrip antenna arrays: (a) Case 1, (b) Case 2, (c) Case 3, and (d) Case 4.

a neutralizing line isolator (Case 2) reduces the coupling between the antennas to a greater extent. In a 2×2 antenna array, the proposed combination reduces the coupling between antennas by more than 6.1 dB. Thus, it will be used in the 25-antenna array.

4. Isolator Design for Twenty-Five-Element Microstrip Antenna Arrays

To further verify the effectiveness of the isolators mentioned above in a large-scale microstrip antenna array, a 5×5 array is constructed, as shown in Figure 10(a), with antennas numbered from 1 to 25. Antenna 13 is situated at the center of the array and has the most complex coupling. Hence, it is chosen as a representative antenna with an active excitation. Without applying the decoupling structures, the simulated and measured S-parameters of the 5×5 antenna array are shown in Figure 10(b). It is seen that the simulated results are consistent with the measured results. The maximum H-plane mutual couplings $|S12, 13|$ and $|S14, 13|$ are −22.3 dB and −22.4 dB, respectively. The maximum E-plane mutual couplings $|S8, 13|$ and $|S18, 13|$ are −20.6 dB and −20.8 dB, respectively.

Since the combination of reversely placed U-shaped line isolators and neutralization line isolators is shown to be effective in Section 3, this combination is implemented for the 5×5 antenna array, as shown in Figure 11(a). The simulated and measured results of the 5×5 antenna array

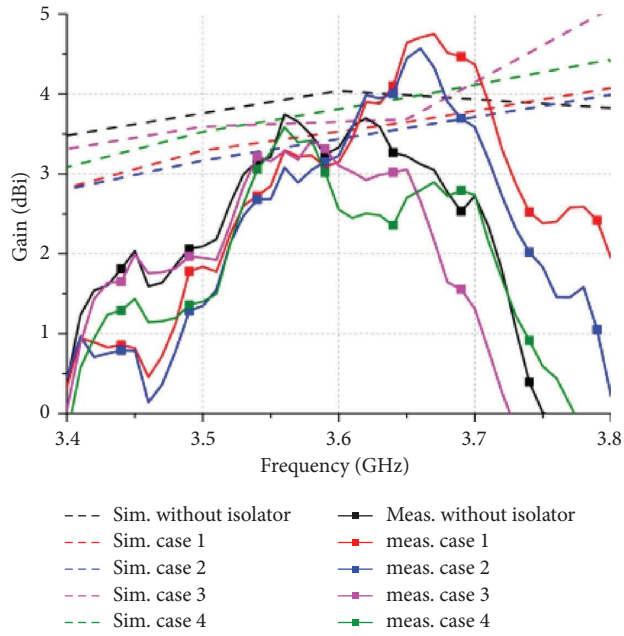

Figure 9: Measured and simulated gains of the microstrip antenna arrays with and without isolators.

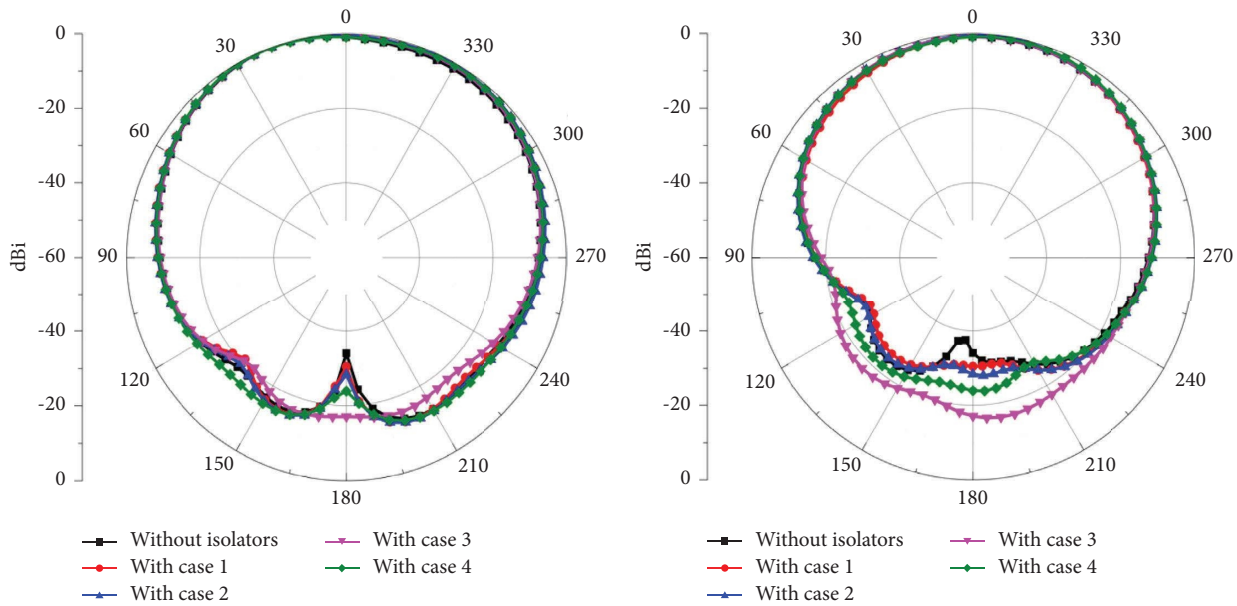

Figure 10: Continued.

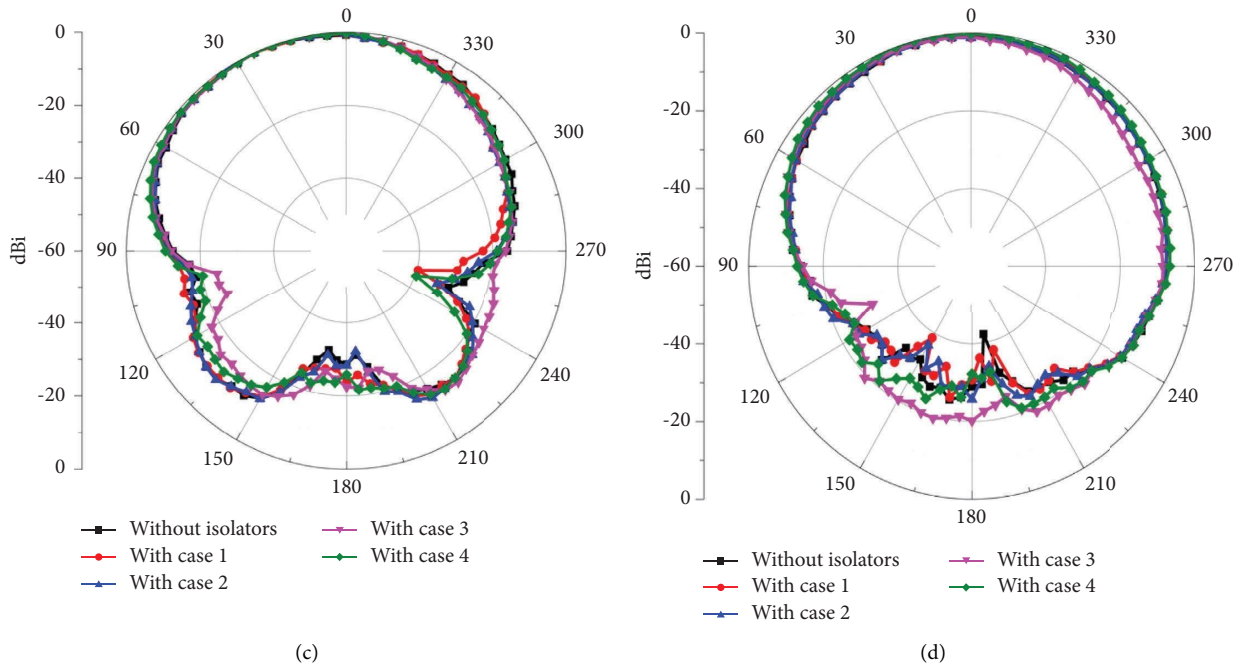

Figure 10: Radiation patterns of 2 × 2 patch antenna array with and without isolators: (a) simulated patterns in the E plane, (b) simulated patterns in the H plane, (c) simulated patterns in the E plane, and (d) simulated patterns in the H plane.

Table 1: *S*-parameters of isolators in the 2 × 2 antenna array.

Antenna array	S21 (dB)	S31 (dB)	S34 (dB)	S24 (dB)	Gain (dBi)	Radiation efficiency (%)
Reference antenna array	−21.6	−22.9	−23.2	−23.0	3.48	52.6
Case 1	−26.9	−28.1	−27.4	−30.0	3.23	46.9
Case 2	−28.7	−29.0	−29.3	−29.1	3.05	48.1
Case 3	−23.6	−27.8	−23.9	−29.6	3.42	53.5
Case 4	−26.3	−28.6	−25.8	−29.2	3.42	54.2

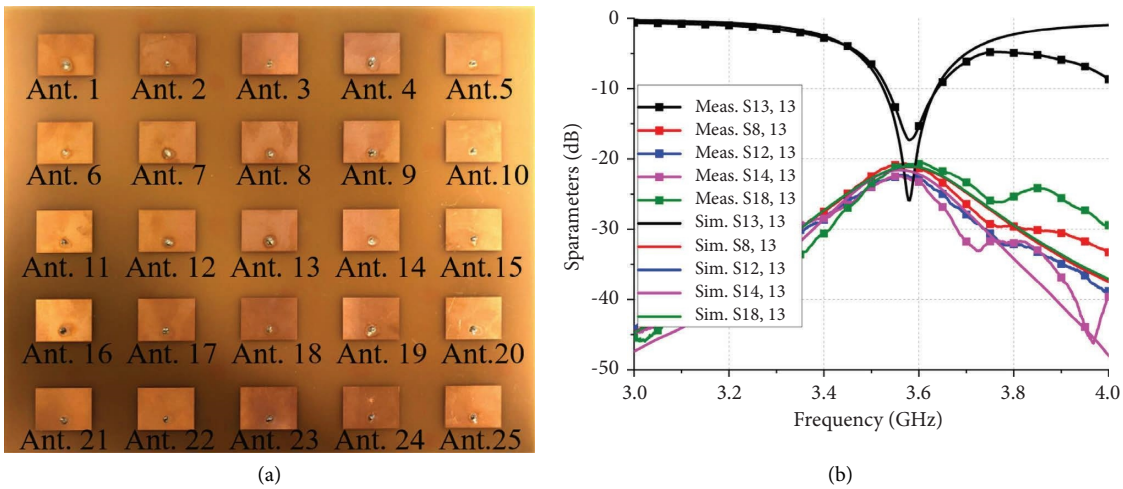

Figure 11: 5 × 5 patch antenna array: (a) fabricated board and (b) simulated and measured *S*-parameters.

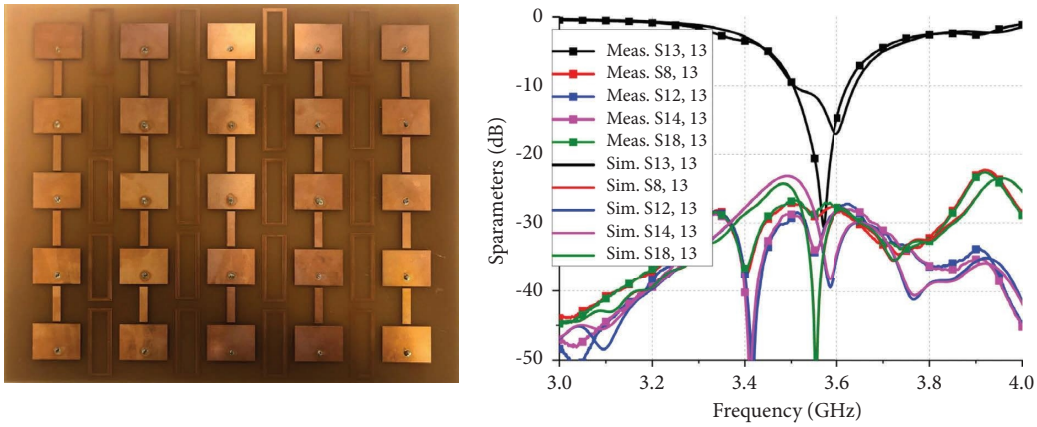

(a) (b)

Figure 12: 5 × 5 microstrip antenna array with isolators: (a) fabricated array, and (b) simulated and measured *S*-parameters.

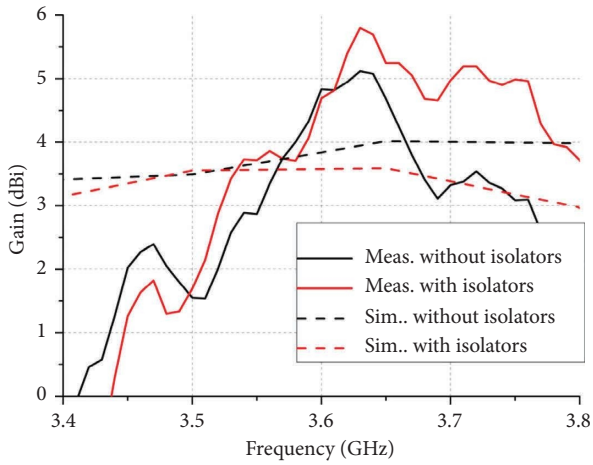

Figure 13: Gains of the 5 × 5 microstrip antenna array with and without symmetrical line isolators.

are shown in Figure 11(b). The measured results agree well with the simulation results. It is noted that the maximum H-plane mutual couplings |*S*12, 13| and |*S*14, 13| are −28.1 dB and −28.2 dB, respectively. The mutual coupling between the horizontal pairs is suppressed by over 5.8 dB. The maximum E-plane mutual couplings |*S*8, 13| and |*S*18, 13| are −27.3 dB and −27.6 dB, respectively. The E-plane coupling is reduced by over 6.7 dB, similar to that in a two-element microstrip antenna array. This, hence, verifies that the isolators' effectiveness is almost independent of the number of antenna elements.

The simulated maximum gain of antenna 13 against frequency is presented in Figure 12 and with and without the isolators are 3.49 dBi and 3.55 dBi, respectively, at the center frequency of 3.5 GHz. However, the measured maximum gain of antenna 13 with the isolators is 3.71 dBi at 3.58 GHz, which is 0.29 dBi lower than that without isolators.

As shown in Figure 13, the radiation patterns with and without isolators are similar, indicating that the isolators only have a small impact on radiation patterns. The simulated radiation efficiency of the antenna 13 without and with isolators is 50.2% and 42.5%, respectively. The isolators reduce the efficiency by only 7.7%.

As shown in Table 2, the proposed isolator shows a relatively low level of gain reduction and acceptable mutual coupling reduction level compared to the previous work, and the mutual coupling reduction levels remain almost constant as the antenna array is varied. In addition, the recent work requires adaptation of the designed isolator to be applied to larger antenna arrays. The proposed decoupler obtains similar isolation enhancement in 2 × 2 and 5 × 5 antenna arrays, verifying that the proposed isolator is almost independent of the number of antennas, which provides an opportunity to apply the designed isolator to large-scale

Table 2: Comparison of the proposed antenna array against the references.

Isolator	Antenna array	Mutual coupling reduction level (dB)	Gain reduction level (dBi)	Modification with antenna array changing
A double-layer meta-surface superstrate [18]	4 × 4	8	NG	Yes
Array-antenna decoupling surface [19]	2 × 2	5	−0.5	Yes
Metamaterial absorber wall [21]	2 × 2	8	−1.2	Yes
Transmission-line-based decoupling structures [23]	4 × 4	8	−0.6	Yes
H-shaped DGS [24]	2 × 2	13	Not given	Yes
Decoupling ground [25]	2 × 2, 4 × 4	7, 7	0.5	Yes
Decoupling slot-strip array [26]	2 × 2, 4 × 4	10, 2	−0.8	No
Neutral lines [28]	2 × 2	3	Not given	Yes
Artificial dielectric layer and metal pillars [29]	4 × 4	5	Not given	Yes
The proposed isolator	2 × 2, 5 × 5	6, 6	−0.3	No

antenna arrays. However, the isolation enhancement level is only over 6 dB over the entire bandwidth, which needs to be improved.

5. Conclusions

This paper comparatively analyzes the mutual coupling between isolators of different types and orientations in a two-dimensional antenna array. Three isolators are proposed in two-port antenna arrays. The U-shaped line isolator and the U-line DGS can reduce the H-field mutual coupling by more than 6.4 dB to below −28.4 dB. The neutralization line obtains about −30 dB of the E-field mutual coupling. Without changing the isolator size, combining the isolator with two reverse-placed line isolators reduces the coupling between the antennas to a greater extent and tunes the isolator performance in the 2×2 microstrip antenna array. The proposed combination reduces the coupling between the antennas by more than 6.1 dB in the 2×2 antenna array and more than 5.8 dB in the 5×5 antenna array. Similar isolation enhancement is obtained, verifying that the proposed isolator is almost independent of the number of antennas. In addition, the introduction of symmetrically arranged U-shaped line isolators has almost no influence on the gain and radiation patterns.

Data Availability

The data used to support the findings of this study are available from the authors on request.

Conflicts of Interest

The authors declare that they have no conflicts of interest.

Acknowledgments

Open Access funding was enabled and organized by JISC.

References

[1] E. G. Larsson, O. Edfors, F. Tufvesson, and T. L. Marzetta, "Massive MIMO for next generation wireless systems," *IEEE Communications Magazine*, vol. 52, no. 2, pp. 186–195, 2014.

[2] S. Asaad, A. M. Rabiei, and R. R. Müller, "Massive MIMO with antenna selection: fundamental limits and applications," *IEEE Transactions on Wireless Communications*, vol. 17, no. 12, pp. 8502–8516, 2018.

[3] I. Singh and V. Tripathi, "Micro strip patch antenna and its applications: a survey," *Int. J. Comp. Tech. Appl*, vol. 2, pp. 1595–1599, 2011.

[4] J. Li and P. Stoica, *MIMO Radar Signal Processing*, John Wiley & Sons, Hoboken, NJ, USA, 2008.

[5] K. S. Vishvaksenan, K. Mithra, R. Kalaiarasan, and K. S. Raj, "Mutual coupling reduction in microstrip patch antenna arrays using parallel coupled-line resonators," *IEEE Antennas and Wireless Propagation Letters*, vol. 16, pp. 2146–2149, 2017.

[6] S. Kharche, G. S. Reddy, R. Gupta, and J. Mukherjee, "Mutual coupling reduction using shorting posts in UWB MIMO antennas," in *Proceedings of the Microwave Conference (APMC), 2016 Asia-Pacific*, pp. 1–4, New Delhi, India, December 2016.

[7] X.-B. Sun and M. Y. Cao, "Low mutual coupling antenna array for WLAN application," *Electronics Letters*, vol. 53, no. 6, pp. 368–370, 2017.

[8] Y. Zhang, J.-Y. Deng, M.-J. Li, D. Sun, and L.-X. Guo, "A MIMO dielectric resonator antenna with improved isolation for 5G mm-wave applications," *IEEE Antennas and Wireless Propagation Letters*, vol. 18, no. 4, pp. 747–751, 2019.

[9] H. Ullah, S. U. Rahman, Q. Cao, I. Khan, and H. Ullah, "Design of SWB MIMO antenna with extremely wideband isolation," *Electronics*, vol. 9, no. 1, p. 194, 2020.

[10] A. Kumar, A. Q. Ansari, B. K. Kanaujia, and J. Kishor, "A novel ITI-shaped isolation structure placed between two-port CPW-fed dual-band MIMO antenna for high isolation," *AEU-International Journal of Electronics and Communications*, vol. 104, pp. 35–43, 2019.

[11] A. Maleki, H. D. Oskouei, and M. Mohammadi Shirkolaei, "Miniaturized microstrip patch antenna with high inter-port isolation for full duplex communication system," *International Journal of RF and Microwave Computer-Aided Engineering*, vol. 31, no. 9, Article ID 22760, 2021.

[12] M. Li and S. Cheung, "A novel calculation-based parasitic decoupling technique for increasing isolation in multiple-element MIMO antenna arrays," *IEEE Transactions on Vehicular Technology*, vol. 70, no. 1, pp. 446–458, 2021.

[13] Z. Yang, J. Xiao, and Q. Ye, "Enhancing MIMO antenna isolation characteristic by manipulating the propagation of surface wave," *IEEE Access*, vol. 8, pp. 115572–115581, 2020.

[14] Z. Wang, C. Li, and Y. Yin, "A meta-surface antenna array decoupling (MAAD) design to improve the isolation performance in a MIMO system," *IEEE Access*, vol. 8, pp. 61797–61805, 2020.

[15] R. Panwar and J. R. Lee, "Progress in frequency selective surface-based smart electromagnetic structures: a critical review," *Aerospace Science and Technology*, vol. 66, pp. 216–234, 2017.

[16] M. Akbari, H. Abo Ghalyon, M. Farahani, A.-R. Sebak, and T. A. Denidni, "Spatially decoupling of CP antennas based on FSS for 30-GHz MIMO systems," *IEEE Access*, vol. 5, pp. 6527–6537, 2017.

[17] S. R. Thummaluru, R. Kumar, and R. K. Chaudhary, "Isolation enhancement and radar cross section reduction of MIMO antenna with frequency selective surface," *IEEE Transactions on Antennas and Propagation*, vol. 66, no. 3, pp. 1595–1600, 2018.

[18] J. Tang, F. Faraz, X. Chen et al., "A metasurface superstrate for mutual coupling reduction of large antenna arrays," *IEEE Access*, vol. 8, pp. 126859–126867, 2020.

[19] K.-L. Wu, C. Wei, X. Mei, and Z.-Y. Zhang, "Array-antenna decoupling surface," *IEEE Transactions on Antennas and Propagation*, vol. 65, no. 12, pp. 6728–6738, 2017.

[20] A. Boukarkar, X. Q. Lin, Y. Jiang, L. Y. Nie, P. Mei, and Y. Q. Yu, "A miniaturized extremely close-spaced four-element dual-band MIMO antenna system with polarization and pattern diversity," *IEEE Antennas and Wireless Propagation Letters*, vol. 17, no. 1, pp. 134–137, 2018.

[21] J. Zhang, J. Li, and J. Chen, "Mutual coupling reduction of a circularly polarized four-element antenna array using metamaterial absorber for unmanned vehicles," *IEEE Access*, vol. 7, pp. 57469–57475, 2019.

[22] Y.-M. Zhang, S. Zhang, J.-L. Li, and G. F. Pedersen, "A transmission-line-based decoupling method for MIMO antenna arrays," *IEEE Transactions on Antennas and Propagation*, vol. 67, no. 5, pp. 3117–3131, 2019.

[23] Y.-M. Zhang, Q.-C. Ye, G. F. Pedersen, and S. Zhang, "A simple decoupling network with filtering response for patch antenna arrays," *IEEE Transactions on Antennas and Propagation*, vol. 69, no. 11, pp. 7427–7439, 2021.

[24] B. Qian, X. Huang, X. Chen, M. Abdullah, L. Zhao, and A. A. Kishk, "Surrogate-assisted defected ground structure design for reducing mutual coupling in 2× 2 microstrip antenna array," *IEEE Antennas and Wireless Propagation Letters*, vol. 21, pp. 351–355, 2022.

[25] S. Zhang, X. Chen, and G. F. Pedersen, "Mutual coupling suppression with decoupling ground for massive MIMO antenna arrays," *IEEE Transactions on Vehicular Technology*, vol. 68, no. 8, pp. 7273–7282, 2019.

[26] D. Gao, Z. Cao, X. Quan, M. Sun, S. Fu, and P. Chen, "A low-profile decoupling slot-strip array for 2× 2 microstrip antenna," *IEEE Access*, vol. 8, pp. 113532–113542, 2020.

[27] S. Farsi, H. Aliakbarian, D. Schreurs, B. Nauwelaers, and G. A. Vandenbosch, "Mutual coupling reduction between planar antennas by using a simple microstrip U-section," *IEEE Antennas and Wireless Propagation Letters*, vol. 11, pp. 1501–1503, 2012.

[28] Y. Li, M. Yuan, Y. Jia, H. Zhai, and C. Liu, "A compact four port MIMO antenna using connected neutral lines for enhanced isolation," in *Proceedings of the 2021 International Conference on Microwave and Millimeter Wave Technology (ICMMT)*, pp. 1–3, Nanjing, China, May 2021.

[29] T. Liu and L. Zhao, "A compact large-scale antenna with high isolation for base station applications," in *Proceedings of the 2021 IEEE International Symposium on Antennas and Propagation and USNC-URSI Radio Science Meeting (APS/URSI)*, vol. 9, pp. 935-936, Singapore, December 2021.